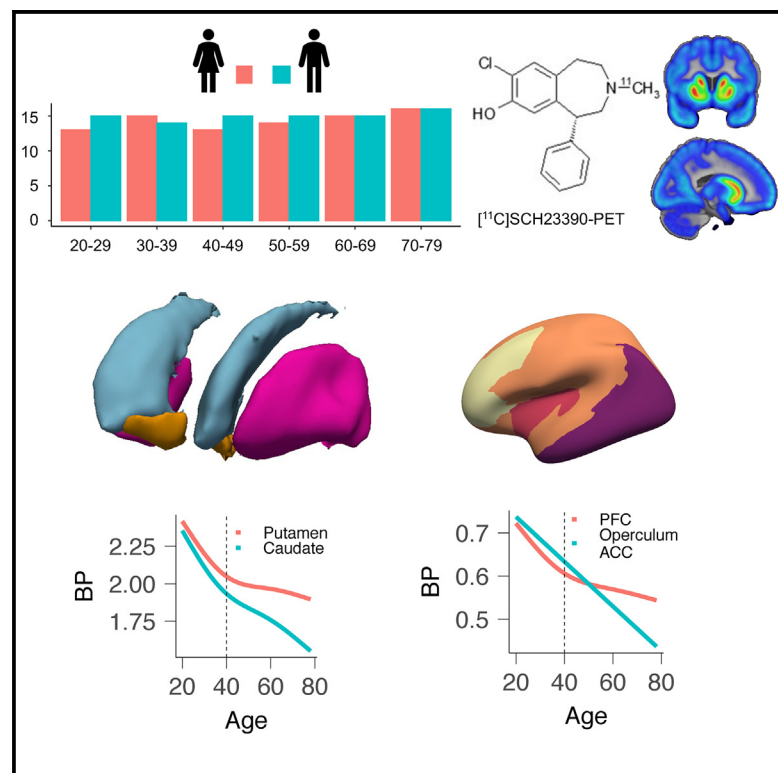


Biphasic patterns of age-related differences in dopamine D1 receptors across the adult lifespan

Graphical abstract



Authors

Jarkko Johansson, Kristin Nordin, Robin Pedersen, ..., Lars Bäckman, Lars Nyberg, Alireza Salami

Correspondence

jarkko.johansson@umu.se

In brief

Johansson et al. identify heterogeneous age-related patterns of D1-like dopamine receptors (D1DRs) across the adult lifespan. In a large sample of healthy men and women, some key regions of the dopamine system, such as the putamen and the prefrontal cortex, exhibit the most dramatic age-related differences during early adulthood (20–40 years of age).

Highlights

- Dopamine D1 receptors (D1DRs) display regionally heterogeneous age patterns across adulthood
- Biphasic age-related pattern is evident in prefrontal cortex and putamen
- Caudate D1DR is strongly linked to white matter lesions in midlife
- D1DR exhibits distinct patterns with neurocognitive function in early vs. late adulthood



Report

Biphasic patterns of age-related differences in dopamine D1 receptors across the adult lifespan

Jarkko Johansson,^{1,2,8,*} Kristin Nordin,³ Robin Pedersen,^{2,4,5} Nina Karalija,^{1,2} Goran Papenberg,³ Micael Andersson,^{2,4} Saana M. Korkki,³ Katrine Riklund,^{1,2} Marc Guitart-Masip,^{3,6} Anna Rieckmann,^{1,2,4,7} Lars Bäckman,³ Lars Nyberg,^{1,2,4,5} and Alireza Salami^{2,3,4,5}

¹Department of Radiation Sciences, Diagnostic Radiology, Umeå University, 90187 Umeå, Sweden

²Umeå Center for Functional Brain Imaging (UFBI), Umeå University, 90187 Umeå, Sweden

³Aging Research Center, Karolinska Institutet & Stockholm University, Tomtebodavägen 18A, 17165 Stockholm, Sweden

⁴Department of Integrative Medical Biology, Umeå University, 90187 Umeå, Sweden

⁵Wallenberg Center for Molecular Medicine, Umeå University, Umeå, Sweden

⁶Max Planck UCL Centre for Computational Psychiatry and Ageing Research, University College London, London, UK

⁷The Munich Center for the Economics of Aging, Max Planck Institute for Social Law and Social Policy, 80799 Munich, Germany

⁸Lead contact

*Correspondence: jarkko.johansson@umu.se

<https://doi.org/10.1016/j.celrep.2023.113107>

SUMMARY

Age-related alterations in D1-like dopamine receptor (D1DR) have distinct implications for human cognition and behavior during development and aging, but the timing of these periods remains undefined. Enabled by a large sample of *in vivo* assessments ($n = 180$, age 20 to 80 years of age, 50% female), we discover that age-related D1DR differences pivot at approximately 40 years of age in several brain regions. Focusing on the most age-sensitive dopamine-rich region, we observe opposing pre- and post-forties interrelations among caudate D1DR, cortico-striatal functional connectivity, and memory. Finally, particularly caudate D1DR differences in midlife and beyond, but not in early adulthood, associate with manifestation of white matter lesions. The present results support a model by which excessive dopamine modulation in early adulthood and insufficient modulation in aging are deleterious to brain function and cognition, thus challenging a prevailing view of monotonic D1DR function across the adult lifespan.

INTRODUCTION

The dopamine (DA) system undergoes profound changes across the lifespan, accompanied by concomitant changes in cognition (see Li et al.,¹ Wahlstrom et al.,² Reynolds and Flores,³ Islam et al.,⁴ and Bäckman et al.⁵ for reviews). In childhood and adolescence, ongoing maturation of the prefrontal DA system is associated with excessive DA activity,^{2–4,6} constraining the development of executive functions.^{7–10} At older ages, DA losses may result in insufficient DA modulation^{11,12} and in decline in multiple cognitive domains.^{5,13–16} Consequently, characterization of age-related DA trajectories holds promise to illuminate the developmental patterns and aging-related deterioration of cognitive function across the lifespan.

During adult life, DA D1- and D2-like receptors (D1DRs and D2DRs, respectively) reduce with advancing age (see Karrer et al.¹⁷ for a review). However, the majority of extant research has focused on extreme age group comparisons precluding precise characterization of age-related trajectories and thus prevents firm conclusions regarding distinct periods of reduction across the lifespan. DA receptors exhibit high expression levels in childhood (2- to 3-fold of adult level) followed by a decline during adolescence.^{18,19} This prolonged developmental process is thought to reflect experience-driven refinement of DA circuitry

to facilitate optimal DA signaling in adulthood.²⁰ In terms of timing of developmental DA receptor elimination, both post-mortem^{21,22} and *in vivo* studies^{20,23} have indicated that the process may continue into young adulthood. Importantly, findings from animal models support the notion that the maturation of presynaptic DA synthesis capacity takes precedence over the protracted elimination of post-synaptic receptors during late development (see Larsen et al.²⁰), resulting in a potentially heightened state of DA modulation. This state of heightened DA modulation, as postulated in Li et al.,¹ may lead to an overstimulated condition that disrupts optimal neural noise suppression, thereby adversely impacting cognitive function. The omission of *in vivo* studies including participants in their middle and late adulthood has, however, left a gap in knowledge about the precise timing of altered DA function. Given the prominent role of DA in neuronal tuning and cognition,¹ and the role of defective DA systems in several psychopathological disorders,²⁴ normative data of lifespan dopaminergic development is needed. Furthermore, the onset of aging-related reductions in DA function must be identified to reliably address the role of DA in normal cognitive aging.^{5,13–16}

Here, we set out to fill this gap in knowledge by investigating the patterns of age-related D1DR differences across the adult lifespan (20–80 years of age) in a large ($n = 180$) age- and



sex-balanced cohort of healthy volunteers using [^{11}C] SCH23390-PET.²⁵ Our focus was on the D1DRs because of their relatively higher cortical abundance compared with other DA receptor subtypes.^{26,27} In addition, despite some indications of a more prolonged developmental trajectory of D1DRs than D2DRs,²² studies investigating age-related differences of D1DRs are remarkably more scarce than those with D2DRs (cf. Karrer et al.¹⁷). The overarching goal was to interrogate the shape of the paths of age-related D1DR differences in order to identify critical ages of transition between distinctive life periods and to explore differences in relation to neurocognitive measures across the putative stages. Two alternative courses of age-related D1DR differences are plausible in view of past findings. Firstly, a linear pattern has been most frequently reported in past studies of D2DR¹⁷ and D1DRs.^{19,28,29} By a monotonous account, it is tacitly assumed that a single neurophysiological mechanism would dominate the influences on D1DR expression across the entire adult lifespan. An alternative view is a non-monotonous pattern, implicating multiple neurophysiological factors (e.g., pruning in early life; vascular deterioration at later adulthood) that have distinct influences across the adult lifespan, similar to those suggested for brain morphology.^{30,31} A non-monotonous pattern may emerge if developmental D1DR elimination in early adulthood is followed by clearly attenuated rates of decline as D1DR pruning wanes. Alternatively, a non-monotonous pattern may emerge if D1DRs display preservation across most of adulthood followed by accelerated rates of decline in older age. Considering the varying rates of age-related alterations observed in structural and functional brain measures, it is plausible that regional heterogeneity in D1DRs may emerge in terms of age-related differences.

Based on prior findings, we hypothesized that (1) most dramatic age-related D1DR differences will be observed in early adulthood, possibly representing prolonged maturation,^{20,23} (2) cerebrovascular integrity may be negatively coupled with D1DR availability in mid to late, but not early, adulthood, in particular in the striatum,^{16,32} and (3) high D1DR levels in early adulthood may reflect an immature DA system (cf. maturational pruning of D1DR), with presumably deleterious implications to neural communication and cognition (cf. Li et al.¹), contrasted by evidence that high D1DRs in middle-aged and older individuals is positively related to measures of brain function and cognition.¹⁵

RESULTS

Spatial distribution of D1DRs across the brain

The spatial distribution of D1DR availability followed the patterns reported previously³³: D1DR binding was highest in striatal regions, followed by frontal, temporal, and parietal regions (Figures 1A and S1). Cortical D1DR binding was approximately five times lower than in the striatum.

Age sensitivity of D1DRs across the brain

Age effects were examined within automatically defined anatomical regions of interest (ROIs) according to the Desikan-Killiany atlas and subcortical structures,^{34,35} providing whole-brain coverage. ROI-based analysis (Figure S2) revealed significant

negative age-related D1DR differences in 87% of the ROIs (Bonferroni-corrected $p < 0.05$, adjusted $r^2 = 0.12$ – 0.63 , mean \pm SD = 0.36 ± 0.12 , percentage of binding potential [BP] difference per decade = $[-8.67, -1.81]\%$, mean \pm SD = -4.58 ± 2.16 ; Table S1), with no hemispheric lateralization of the age effects (paired t test $p = 0.45$, interhemispheric correlation Pearson's $r = 0.8$; Figure S3). The bilateral hippocampus, the amygdala, the entorhinal cortex, the unilateral pallidum, and the lateral occipital cortex were absent of age effect (Table S1), and these regions were hence excluded from further analyses. Together, these results suggest widespread age-related reductions to D1DRs across the brain.

Age-related D1DR differences are non-monotonous across the adult lifespan

Hierarchical generalized additive models (GAMs) were run on the cortical ROIs in order to reduce the number of ROIs exhibiting mutually similar relationships with age (see supplemental information). This analysis identified four composite cortical ROIs (Figure 1B; Tables S2–S4), the prefrontal cortex (PFC), the operculum and anterior cingulate cortex (ACC), and the posterior and central cortices, that were entered in the subsequent analysis, together with the three anatomical subregions of the striatum (the caudate nucleus, the putamen, and the nucleus accumbens; cf. Figure 1B).

Model comparison using Akaike information criteria (AICs)³⁶ was used to identify the best age model fit. Log-transformed regional D1DR age differences were best explained by a non-linear GAM in all ROIs except in the caudate and the operculum and ACC (Table 1; ΔAIC range = 2–13), indicating non-linear age-related effects in putamen, PFC, central and posterior cortices, and nucleus accumbens D1DRs. Notably, log transformation of the D1DR scores ensured that the non-linearities were not due to monotonous exponential decay—as suggested in some past studies.^{23,29}

In accordance with a non-monotonic pattern of age-related differences, visual inspection of GAM predictions suggested discernible attenuation of D1DR reductions around age 40 years (Figure 1C; see Figure S4 for data not corrected for partial volume effect [PVE]). Furthermore, inspection of the GAM predictions revealed overlapping and differing regional age patterns before and after approximately 40 years of age, respectively (Figures 1D and 1E). Specifically, overlapping age-related patterns of caudate and putamen D1DRs were observed in early adulthood, contrasted by clearly larger caudate than putamen D1DR reductions in middle-to-late adulthood (Figure 1E).

Statistical interrogation of local changes in the patterns of age-related D1DR differences were conducted using second-order derivatives of regional GAM predictions.³⁷ Second-order derivatives revealed a significant peak (Figure 1F) at approximately 35–40 years of age in the putamen and the PFC. Furthermore, visual analysis suggested that interregional differences in the rates of difference were primarily manifested after the age of 40 years (Figures 1C–1E).

Statistical analysis of a changing rate of D1DR reductions before and after the putative critical age of 40 years was next conducted using a bilinear model, incorporating different age-related slopes in early (age 20–40 years) vs. later adulthood

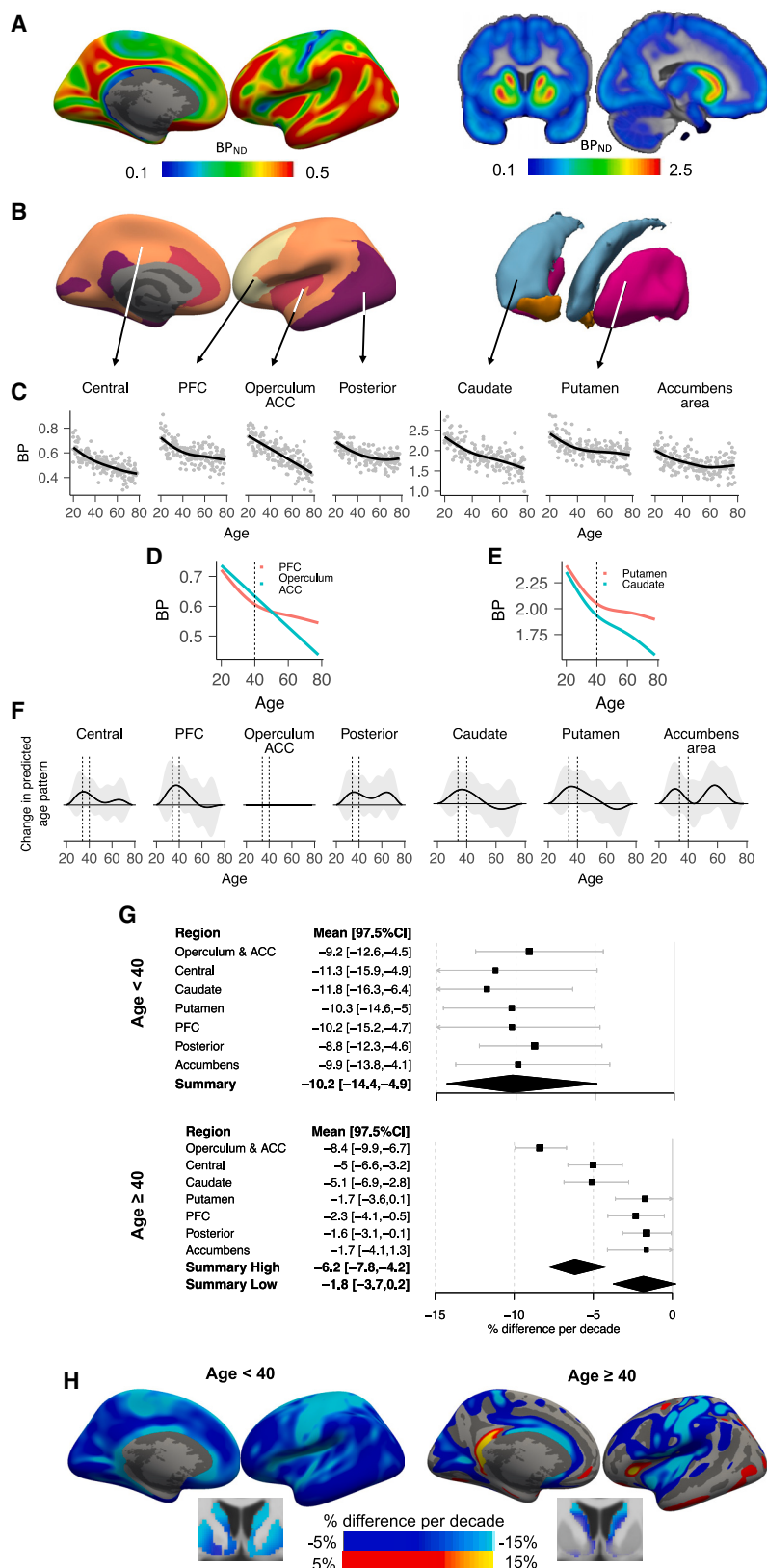


Figure 1. Age-related differences in [^{11}C] SCH23390 BP_{ND} across the adult lifespan

(A) Spatial distribution of D1DRs in the cortex (left) and deep brain structures (right).

(B) Cortical regions of interest (ROIs) based on similar age-related trajectories within Desikan-Killiany parcellation (left). Anatomical ROIs in the striatum (right).

(C) Scatterplots represent ROI-wise D1DR availability in relation to age; solid lines represent GAM predictions.

(D) Overlay of PFC and cingulo-opercular GAM predictions, highlighting regionally divergent patterns from approximately 40 years of age (dashed line).

(E) Same as (D) but between putamen and caudate.

(F) Changes in age-related GAM predictions were assessed using second-order derivatives. The putamen, the PFC, and the caudate indicated a peak at approximately age 35–40 years of age (dashed vertical lines), providing statistical evidence of non-monotonic age trajectories in the putamen and the PFC (cf. 95% CI).

(G) D1DR percentage of difference per decade (see STAR Methods) for participants younger (top) and older (bottom) than 40. Bootstrapping ($n = 500$) was used for estimation of mean (box) and 95% CI (whiskers) of percentage of difference per decade. Non-overlapping CIs were interpreted as significant rate differences ($p < 0.05$).

(H) Maps of voxel-wise percentage of difference per decade for participants younger (left) and older (right) than 40.

Table 1. Akaike information criteria (AICs) scores of regional models of D1DR age trajectories

	AIC score		
	Linear	GAM	Bilinear
Putamen	−289	−297 ^a	−299 ^a
Caudate	−203	−202	−204 ^a
Accumbens	−198	−205 ^a	−202 ^a
PFC	−247	−252 ^a	−253 ^a
Operculum and ACC	−217 ^a	−216	−215
Central	−255	−257 ^a	−257 ^a
Posterior	−305	−318 ^a	−316 ^a

Log-transformed D1DR availability served as dependent variable to account for putative constant relative rates of decline (exponential decay model). Linear model with constant slope across the adult lifespan served as a reference model. General additive model (GAM) allowed for assumption-free analysis of non-linear age effect. A biphasic linear model incorporating different slopes of age-related differences in early (age 20–40 years) vs. later adulthood (age ≥ 40 years) assumes a change in the slopes at a particular age (40 years of age). Lower AICs indicated a superior model fit.

^aImproved data fit relative to a linear model.

(age ≥ 40 years). A bilinear model outperformed a constant linear model in all regions, including the caudate, except in the operculum and ACC (Tables 1 and S5). Lower or equal AICs compared with GAM in the caudate, the putamen, the PFC, and the central cortex (Table 1) suggest that 40 years was a critical age in these regions. In contrast, lower AICs of GAM in the accumbens and the posterior cortex (Table 1) suggest that the putative inflection was not greatest at age 40 but possibly at some later age (cf. Figure 1C).

Bilinear model with bootstrapping (n = 500 replicates) was then used to estimate the percentage of D1DR differences per decade (±97.5% confidence intervals [CIs]) within the two age segments. In the putamen, the nucleus accumbens, the PFC, and the posterior cortex (Figure 1G), non-overlapping 97.5% CIs were observed, suggesting statistically significant differences in the effects of age before and after the forties, after controlling for false discovery rate (FDR). This post-forties regional heterogeneity in the effects of age was used to identify two sets of regions exhibiting dissimilar effects of age. The first included the operculum and ACC, the caudate, and the central cortex, characterized by continued negative post-forties D1DR age differences (mean [97.5% CI] = −6.2% [−7.8, −4.2]), in contrast to the second set of regions including the putamen, the PFC, the posterior cortex, and the nucleus accumbens exhibiting non-significant post-forties age effects (mean [97.5% CI] = −1.8% [−3.7, 0.2]). Notably, the 97.5% CIs of the two groups of regions were not overlapping, indicating significant interregional heterogeneity in the effects of age post-forties. In contrast, in early adulthood, the cross-regional estimates of the percentage of D1DR difference per decade were within 3 percentage units, and all 97.5% CIs were overlapping, indicating regionally homogeneous effects of age (Figure 1G; non-overlapping 97.5% CIs). Collectively, the bilinear analyses suggested regionally overlapping effects of age in pre-forties but not in

post-forties. A converging pattern was revealed using voxel-wise bilinear analysis (Figure 1H), suggesting brain-wide D1DR decrements in pre-forties, contrasted by limited areas of significant age-related differences in post-forties.

Cerebrovascular integrity is more strongly coupled with caudate than putamen D1DRs

We next investigated a hypothesis by which the post-forties D1DR age differences were influenced by deleterious consequences of aging, in contrast to putative predegenerative effects in early adulthood. Our primary focus was on the caudate and the putamen because of the interregional differences of the post-forties age effects across the two regions (Figure 1E) as well as a previously identified cerebrovascular risk factor for dopaminergic decline in the striatum.^{16,38} In particular, we tested a hypothesis by which the interregional differences between caudate and putamen D1DRs may be related to distinct regional influences of white matter lesions (WMLs),³⁹ an early marker of brain aging.

Across the entire sample, WML volumes ranged between 0 and 27 mL, with negligible WML manifestation in early adulthood (volume range 0–1.2 mL, n = 60). In keeping with the notion that WML manifestation represents vascular health,⁴⁰ an age-corrected association was found between the Framingham Risk Score⁴¹ and the log-transformed WML volumes (age partial correlation = 0.17, p = 0.035). In post-forties (n = 116), the log-transformed WML volume was more strongly coupled with caudate than with putamen D1DRs (Figure 2A; age partial correlations: $r_{\text{caudate}} = -0.39$, p < 0.01; $r_{\text{putamen}} = -0.21$, p = 0.03, William's test for difference in dependent correlations $t = -12.48$, Bonferroni-corrected p < 0.01; Table S6). Accordingly, statistical adjustment for the effect of WML resulted in a more dramatic change in the GAM prediction of the caudate than the putamen D1DR trajectory (Figure 2B). Critically, visual inspection of the GAM predictions suggested clearly discernible pivots at approximately age 40 in the age patterns of caudate D1DRs after adjustment for WML volume (Figure 2B). Furthermore, using linear mixed-model comparisons (see Table S7), statistical support for overlapping shapes of D1DR age patterns between the caudate and the putamen was found after adjustment for the effects of WML. Hence, we concluded that in the caudate, waning of the late developmental reorganization—at approximately age 40 years—may not have been temporally very distal with the early manifestations of degenerative events, effectively masking the transition between phases (Figure 2C).

Additional analyses were conducted, including on the accumbens area and cortical D1DR availability. The associations between lesions and D1DRs in these regions were found to be significantly weaker ($r = -0.10$ to -0.24 ; p = 0.29 to 0.015) as compared with the caudate D1DR-lesion association (William's test for difference in dependent correlations, Bonferroni-corrected p < 0.01; Table S6). Taken together, all regions showed significantly weaker age partial correlations between WML and D1DR compared with the caudate.

Associations between D1DRs and neurocognitive function are moderated by age segment

We next investigated age-moderated relationships between D1DRs and neurocognitive measures. Here, we focus on the

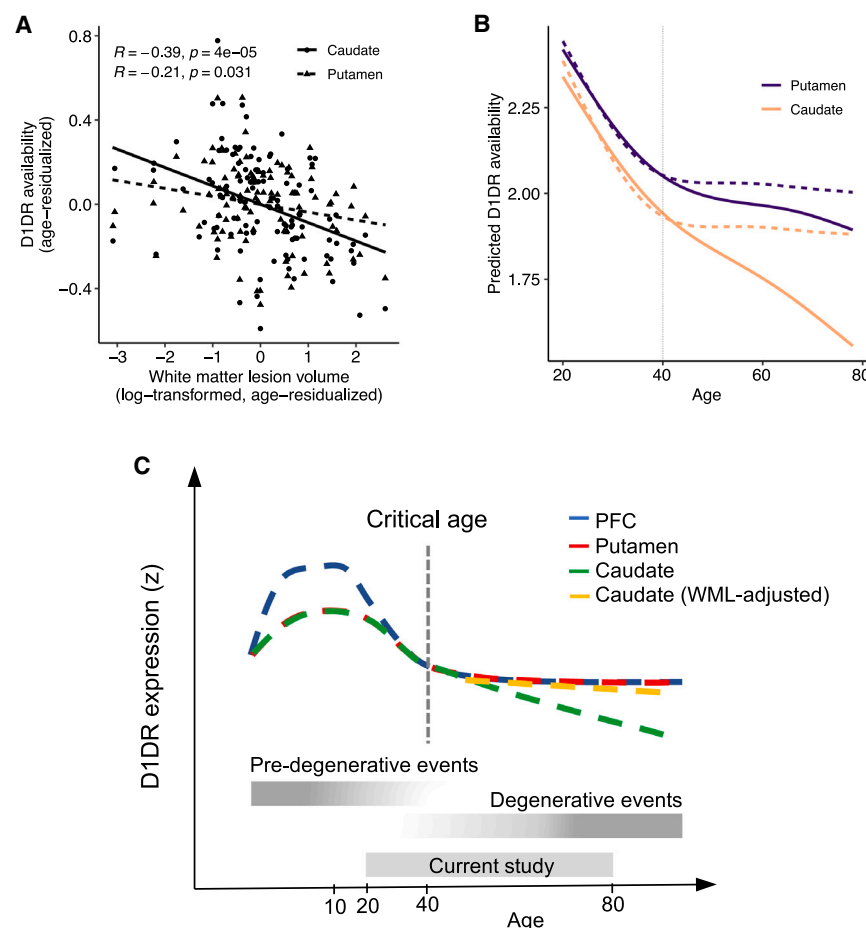


Figure 2. Regionally distinctive relations between D1DR availability and cerebrovascular burden (WML volume)

(A) Scatterplot showing a stronger partial correlation between caudate than putamen D1DRs and WML volume.

(B) Predicted age trajectories of putamen and caudate D1DR availability. Interregional differences in age-related trajectories of raw data (solid lines) were abolished after adjustment for the region-specific effect of WML volume (dashed lines). (C) A hypothetical model for biphasic age-related D1DR trajectories. This simplified cartoon represents how two overlapping neurophysiological events can shape the age trajectories in different brain regions and how timing of critical age may reflect the transition from one phase to another. In early parts of life, D1DR expression may increase, caused, for instance, by normal developmental proliferation and synaptic arborization. In the case of development, waning of developmental events affects the rates of change, detected as a change in second derivative and termed here as critical age (dashed gray line). In this scenario, transition between events is more pronounced in the PFC and the putamen as compared with the caudate, where the onset of degenerative events overlaps with the end of predegenerative events. Exclusion of cerebrovascular insults indexed by WMLs realigned the age trajectory in the caudate to match with the pattern in the putamen.

most age-sensitive DA-rich region, the caudate, given its ubiquitous connection, via the cortico-caudate circuit, with the associative cortex^{42,43} and its implication for functional connectivity and higher cognitive function, such as memory.^{44,45} The primary aim of the present analysis was therefore to test the hypothesis that caudate D1DR differences during early and late adulthood have distinct implications for brain function and cognition.¹

Caudate D1DRs in relation to memory across the adult lifespan

Given the established role of caudate DA in both episodic and working memory processing,^{45,46} we focused on a composite memory score (see STAR Methods). Similar to caudate D1DRs, a non-linear trajectory across the adult lifespan was observed for composite memory score (Figure S5). Using multilinear regression, we found a main effect of caudate D1DRs with no evidence for differential pre- and post-forties implications to memory (D1DR effect $t = 2.61$, $p = 0.009$; D1DR \times [age < 40] interaction effect $t = -0.58$, $p = 0.56$). Additional bilinear analysis (Figure 3A), however, suggested a positive D1DR-memory relationship in middle to late adulthood ($r_{Age \geq 40} = 0.43$, $p < 0.001$; age partial $r_{Age \geq 40} = 0.24$, $p = 0.009$), whereas no such association was observed in pre-forties ($r_{Age < 40} = 0.14$, $p = 0.32$),

speaking to a potentially moderated effect of D1DR on memory in early adulthood. A follow-up voxel-wise analysis revealed significant linear D1DR-memory

Caudate functional connectivity in relation to memory across the adult lifespan

Strength of functional cortico-caudate connectivity (see STAR Methods) was positively related to age, and no moderation by age segment was found (age effect $t = 3.02$, $p = 0.003$; age \times [age < 40] interaction effect $t = -0.57$, $p = 0.55$), in accord with hypothesis by which connectivity strength increases during late development as well as in aging (see Figure S6). Notably, distinct implications of cortico-caudate connectivity to memory during pre- and post-forties was found (functional connectivity [FC] effect $t = -2.05$, $p = 0.041$; FC \times [age < 40] interaction effect $t = 2.43$, $p = 0.017$, $\Delta R^2 = 0.02$, $p = 0.03$). Follow-up analysis (see Figure S7) corroborated a negative memory-cortico-caudate connectivity relationship in late adulthood ($r_{Age \geq 40} = -0.32$, $p < 0.001$; age partial $r_{Age \geq 40} = -0.19$, $p = 0.04$), whereas only a positive trend was observed in early adulthood ($r_{Age < 40} = 0.21$, $p = 0.11$). A group-wide negative memory effect of cortico-caudate connectivity in midlife and beyond concords with the hypothesis that elevated cortico-caudate connectivity may have negative consequences for cognition in aging.^{47,48}

Caudate D1DRs in relation to cortico-caudate connectivity across the adult lifespan

We next test the hypothesis that caudate D1DRs exhibit opposing associations with caudate FC during early and late adulthood. In support of our hypothesis, differential links between caudate D1DRs and cortico-caudate connectivity were observed during pre- and post-forties (D1DR effect $t = -3.31$, $p = 0.001$; D1DR \times [age < 40] interaction effect $t = 2.42$, $p = 0.02$, $\Delta R^2 = 0.062$, $p = 0.007$). Further, bilinear analysis (see Figure S8) corroborated that lower D1DRs were related to higher cortico-caudate connectivity in late adulthood ($r_{Age \geq 40} = -0.36$, $p < 0.001$; age partial $r_{Age \geq 40} = -0.28$, $p < 0.001$), while no direct association was observed in early adulthood ($r_{Age < 40} = -0.01$, $p = 0.92$). Taken together, our results suggest that lower caudate D1DRs in older age were associated with elevated cortico-caudate connectivity, which was in turn linked to less-efficient memory function in older age.

Caudate D1DR, cortico-caudate connectivity, and memory across the lifespan

The results so far revealed age-differential implications of D1DR to cortico-caudate connectivity and of cortico-caudate connectivity to memory, but no significant association was found in early adulthood alone. Here, we interrogated the possibility that neurocognitive associations in early adulthood were further moderated by individual differences, possibly reflecting heterogeneity in neural maturation.⁴⁹ That is, some individuals may show more advanced, and others exhibit more delayed, stages of D1DR maturation, potentially contributing to mixed patterns in relation to neurocognitive measures. To this end, we considered FC as a proxy for neural signal-to-noise ratio and examined whether D1DRs in different age segments and at different levels of cortico-caudate connectivity would exhibit distinct relations to memory (i.e., immature state of DA development: high D1DR concomitant with low FC in early adulthood). First, the hypothesis of distinct pre- and post-forties compound effects of caudate D1DRs and cortico-caudate connectivity on memory was investigated. Notably, a significant three-way interaction effect (D1DR \times FC \times [age < 40] effect $t = 2.66$, $p = 0.009$) corroborated that the compound implication of caudate D1DRs and cortico-caudate connectivity for memory altered as a function of age segment. Further age-split analysis revealed a coherent positive effect of caudate D1DRs ($t = 2.17$, $p = 0.03$) but not FC ($t = -1.48$, $p = 0.14$) to memory after age 40, suggesting that regardless of FC level, older individuals with higher D1DRs exhibited more efficient memory processing (Figure 3C). In contrast, in early adulthood, inclusion of an interaction between D1DRs and connectivity was critical for explaining memory differences (memory \sim D1DR + FC, $R^2 = 0.07$, not significant [n.s.]; memory \sim D1DR + FC + D1DR \times FC: $R^2 = 0.18$, $p = 0.02$, D1DR effect $t = 2.38$, $p = 0.02$, FC effect $t = 0.10$, n.s., D1DR \times FC effect $t = 2.59$, $p = 0.01$; age < 40 years of age, $n = 56$; see Figure 3C). Different patterns of D1DR-memory relation for high and low cortico-caudate connectivity indicated that high D1DR availability in early adulthood, when concomitant with low cortico-caudate connectivity (below median), was not beneficial to memory (Figure 3D), contrasted by positive implications of high D1DR availability in older age when concomitant with high cortico-caudate

connectivity (above median, Figure 3C). Follow-up analyses using cortico-putamen FC revealed a similar pattern as for the caudate, suggesting that both of these DA-rich regions concurred in exhibiting opposing relationships with neurocognitive measures across the adult lifespan (supplemental information). However, unlike the cortico-caudate-D1DR relationship, the cortico-putamen-D1DR link was not moderated by age segment.

Further follow-up analysis in the PFC, in relation to frontoparietal connectivity (see STAR Methods) and working memory, were conducted (supplemental information). The hypothesis was that D1DRs in the PFC—showing a marked age-related pivot at approximately age 40—may have distinct implications for cortico-cortical FC and cognition across the age segments, in a similar manner as in the caudate. To that end, a negative effect of D1DRs to frontoparietal FC was observed in the young, in line with a hypothesis that high PFC D1DRs during development may contribute to lower signal-to-noise ratio and connectivity.^{1,50} No direct or interaction effects between PFC D1DRs and memory were observed.

DISCUSSION

Unlike prevailing accounts of monotonic dopaminergic decline, the present study provides *in vivo* evidence of a biphasic pattern of age-related D1DR differences across the adult lifespan. An inflection point in the pattern of D1DR age differences provided tentative evidence for a qualitative distinction between reductions in early and late adulthood. Importantly, using data-driven identification of local changes in the pattern of age-related D1DR differences,³¹ direct statistical support for a critical age at approximately 35–40 years of age was found (Figure 1F). Moreover, bilinear analysis indicated significantly higher rates of reduction during pre- than during post-forties in several brain regions, including the putamen, the nucleus accumbens, and the PFC (Figure 1G). The finding of more dramatic reductions in early adulthood coheres with past *in vivo* lifespan studies showing quadratic and bilinear age patterns of D2DRs.^{51,52}

The patterns of regional age-related D1DR differences were primarily characterized by cross-regional similarity in early, but by regional variability in late, adulthood. This resonates well with cross-regional synchrony of developmental events^{18,53} and with regionally specific susceptibility to aging-related events in later life (e.g., ladecola⁵⁴), respectively. A multifactor model of D1DR alterations across the adult lifespan, similar to those proposed for brain morphology^{30,31} and connectivity,^{55,56} may hence offer a biologically plausible account of the present findings and lay foundation for an account of the spatial dynamics of age-related D1DR differences across the adult lifespan.

In contrast to a multifactor model, the currently prevailing unimodal account tacitly assumes the predominance of a constant aging-related mechanism of DA receptor losses across the adult lifespan. Speaking against the unimodal account, we show that age-related D1DR reductions in a number of regions—most strikingly, those of the putamen and the PFC—decelerated in midlife (Figure 1F). This is in apparent discord with typically accelerating—not decelerating—rates of age-related decline for cognition and brain integrity in aging.^{31,57–59} To that end, our findings of a moderate rate of D1DR differences in midlife

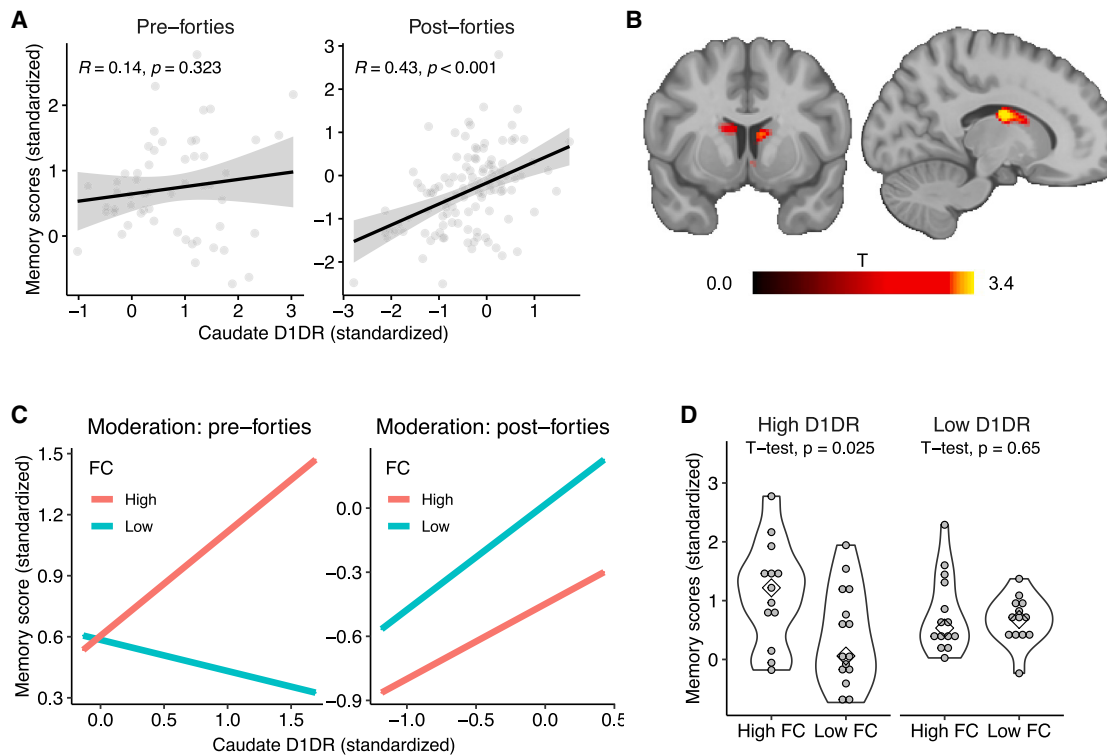


Figure 3. Non-linear interrelations among age, caudate D1DRs, cortico-striatal FC, and memory

(A) Age-moderated caudate-D1DR-memory relation (Pearson's R).

(B) Statistical parametric maps (t value of linear regression model) of D1DR-memory association in older adults (age ≥ 40 , $n = 113$). Two clusters ($p < 0.01$, uncorrected, cluster forming threshold $k = 50$) were detected in the left (peak: $-14, -6, 16$) and the right (peak: $14, -6, 22$) dorsal caudate.

(C) In early adulthood (age < 40 , $n = 55$), caudate D1DRs and strength of cortico-caudate connectivity interacted to influence memory scores ($t = 2.59$, $p = 0.01$). The conditional tendency of caudate D1DRs to memory was positive for high cortico-caudate connectivity (red, 1 SD above the mean) and negative for low cortico-caudate connectivity (cyan, 1 SD below the mean). For older adults (age ≥ 40 , $n = 113$), no interaction between caudate D1DR and cortico-caudate connectivity in relation to memory was observed (see main text).

(D) In early adulthood ($n = 55$), high caudate D1DRs (above median) when accompanied by low cortico-caudate FC (below median) were associated with poorer memory than when concomitant with high cortico-caudate FC (above median). No memory difference was observed among participants with low caudate D1DRs (below median).

and beyond (mean = -3.7% ; Figure 1G) differ from the general pattern estimated in past imaging studies (mean = -14% ; for a review, see Karrer et al.¹⁷) but are in a good agreement with post-mortem investigations (mean = -4% per decade)^{19,28} and with imaging studies where non-linear age models were investigated.^{51,52} Furthermore, longitudinal investigation of D2DR change in elderly (>65 years of age) concurs with the present findings suggesting an approximately 4%–5% decline per decade in the striatum.³² Collectively, this pattern of findings suggests that the magnitude of age-related D1DR differences may have been overestimated in midlife and beyond when using linear age models. In addition, whole-brain mapping of age effects revealed that age-related differences were highest for the operculum and ACC ($\sim 8\%$), moderate in the caudate and the central cortex ($\sim 5\%$), and weakest in the accumbens, the putamen, the PFC, and posterior regions ($\sim 2\%$). Stable D1DR expression across the adult lifespan was observed in several regions, including the hippocampus, the amygdala, and the entorhinal cortex. The observed stability of hippocampal D1DRs is consistent with previous studies reporting stable hippocampal

D2DR levels throughout adulthood⁵¹ (but see Karalija et al.³²). Taken together, our results suggest that across the adult lifespan, many regions exhibit non-linear age-related D1DR patterns. However, there are also regions that display linear patterns, and interestingly, certain regions show no age-related differences at all. In accord with the present findings, Seaman and colleagues⁵¹ found regional heterogeneity in the age-related patterns of D2DRs, such that in several regions, including the putamen and the PFC, D2DR availability declined from young adulthood to middle age and then was relatively stable until old age, whereas in other regions, such as the caudate, a linear pattern was observed (Figure 3). Despite the diminished estimates of D1DR losses in aging, some of which are not statistically significant in key regions, the current findings suggest that degeneration of D1DRs occurs post-forties, aligning with the proposed role of DA in cognitive aging.¹⁵ This is supported by the association between lower D1DR levels and impaired functional communication, leading to poorer memory function post-forties. Additionally, our recent study demonstrated that older individuals with greater D1DRs exhibit less dedifferentiation of the

functional connectome and more efficient working memory.⁶⁰ Overall, the notion of greater D1DRs as a resilience mechanism is compelling and reinforces the idea that DA markers may play a pivotal role in neurocognitive decline. Finally, the onset age of degenerative D1DR differences proposed here are closer to typical onset ages of decline for some cognitive domains,^{58,59} and the regions affected by aging-related decline—particularly the caudate and the cingulo-opercular cortex—are strongly implicated in higher cognitive function.

Offering further support for a dichotomy between pre- and post-forties reductions, we identified a likely mechanism of D1DR reduction that was only present during midlife and beyond. In particular, caudate, more so than putamen, D1DRs were negatively coupled to manifestation of WMLs in post-forties (Figure 2A), and critically, statistical adjustment for the regionally disparate effects of WMLs—a hallmark of cerebral small-vessel disease—abolished differences in the age-predicted trajectories of caudate vs. putamen D1DRs (Figure 2B). This finding lends itself to two notable conclusions: first, coupling of caudate D1DR reduction in aging with WMLs—which were absent during early adulthood—suggests a specific, deleterious cerebrovascular pathway to caudate D1DR reductions in late adulthood. Second, overlapping timing of D1DR reductions across the caudate and the putamen—after adjustment for disparate aging-related consequences—adds evidence for similar timing of predegenerative events across several brain regions. The proximity of the caudate to the typical manifestation sites of WMLs (e.g., corona radiata) may have contributed to its specific susceptibility relative to other D1DR-rich brain regions. Accordingly, the present results suggest that WMLs did not significantly impact prefrontal D1DRs, despite some previous research indicating particular vulnerability of the PFC to the deleterious effects of WMLs.⁶¹ It is plausible that this finding may also reflect a relatively low burden of WMLs in the DyNAMiC cohort (0–27 mL). Possibly, as lesions expand, DA integrity in other brain regions may also be affected.³² Finally, relatively low spatial resolution of the FLAIR data used for WML estimation may be considered a methodological limitation. However, it is important to highlight that the lesion growth algorithm (LGA) has shown reliable performance even with low-resolution FLAIR.⁶² Although it remains unclear whether elevated WML manifestation is the cause or the consequence of dopaminergic alterations in aging, the current finding, along with the observations of longitudinal change–change association between D2 and WMH,³² suggests a tight coupling between DA and cerebrovascular integrity.

The present study shows non-linear relationships between neurocognitive function and D1DRs, coherent with a dichotomy between pre- and post-forties effects to D1DR availability across the adult lifespan. In keeping with late maturation of caudate D1DR, the association between caudate D1DR and memory was moderated by cortico-caudate connectivity (a potential indicator of DA modulation of neural communication) in early adulthood (Figure 3C). Specifically, low cortico-caudate connectivity when accompanied by high D1DR levels, possibly reflecting excessive DA–D1DR modulation, was associated with lower memory function. In contrast, younger adults with higher cortico-caudate connectivity were more efficient in memory pro-

cessing and, importantly, exhibited the expected positive association between D1DRs and memory. A similar age-differential association was also observed between PFC D1DRs and fronto-parietal connectivity and between striatal D1DR and cortico-putamen connectivity, indicating a replicable pattern of interrelations among D1DR, FC, and age across the brain. Past research has suggested a negative relation between increased striatal FC and cognition in aging,^{47,48} which was observed also here in middle-aged and older participants. Furthermore, a negative association between caudate D1DRs and strength of cortico-caudate connectivity in aging, together with prior findings of elevated BOLD variability with aging-related D1DR losses,⁶³ suggests dopaminergic underpinnings to a deleterious aging-related increase of cortico-striatal connectivity. Given the well-established parallel loop organization of connections from the cortex to the striatum,⁶⁴ and past reports of aging-related dedifferentiation of cortico-caudate connectivity,⁶⁵ a plausible mechanism is that decreased levels of caudate DA–D1DR modulation may contribute to increased cross-talk across segregated functional networks. Although the associations between D1DR and neurocognitive function were more pronounced in older adulthood, our overall findings are in keeping with an inverted-U-shaped model of lifespan differences in DA modulation (e.g., Li et al.¹) and are akin to past findings suggesting non-linear, age-moderated interrelations between DA, fMRI-BOLD, and cognition across the adult lifespan.^{66–68} While we proposed a tentative model that differences in D1DR pre- and post-forties are distinct and may reflect developmental and age-related alterations, it is crucial to validate this model with longitudinal data to further elucidate neurophysiological underpinnings of D1DR changes occurring at different stages of life.

Limitations of the study

Tight regulatory coupling has been suggested among the various components of the dopaminergic system (i.e., synthesis capacity, receptor balance, reuptake efficiency; cf. Sulzer et al.⁶⁹). For instance, in the early stages of Parkinson's disease, upregulation of DA receptors has been suggested as a compensatory response to declining extracellular DA levels.⁷⁰ Furthermore, accumulating evidence suggests that normal aging is associated with upregulated DA synthesis, possibly in response to DA receptor losses.^{71,72} Therefore, firm conclusions about extensive or insufficient DA modulation are not reached via quantification of a single dopaminergic marker. To date, non-linear age effects have been detected in D2DR availability,^{51,52} while a unique large-scale investigation found no evidence for non-linear age effects for DA transporters (DATs) across the adult lifespan.⁷³ Together with the indications of non-linear age trends for D2DR but not for DATs in a large meta-analysis,¹⁷ the evidence speaks for a potential dichotomy between pre- and post-synaptic effects of age, in line with the hypothesis that presynaptic DA markers may precede the maturation of post-synaptic DA receptors.²⁰ At present, there are a lack of human *in vivo* studies representing multiple aspects of dopaminergic maturation and aging in the same participants across the adult lifespan. Although the dynamic sample size is about 10 times as large as a typical DA PET study,¹⁷ the smaller number of young participants (*n* = 55) in the analyses of FC-moderated association between

D1DR and memory should be considered in any interpretation of these findings. Although it is encouraging that moderation effects were consistent for analyses considering cortico-caudate and cortico-putamen FC separately, the results must be interpreted with caution while pending replication, preferably using longitudinal setting. A further limitation is related to the affinity of [^{11}C]SCH23390 to not only D1DR but also to serotonin receptors of subtype 2A (5HT-2AR).⁷⁴ Expression of 5HT-2AR is low in the striatum⁷⁵ but may significantly contribute to [^{11}C]SCH23390 binding in the cortex. Relatedly, the age-related pattern of global cortical 5HT-2AR⁷⁶ mirrors the pattern observed for PFC D1DRs, suggesting that the two targets may show similar age differences across the lifespan. At present, the unique age-related pattern of cortical D1DRs across the lifespan remains poorly characterized.

In conclusion, the present findings suggest a multifactor model of age-related D1DR differences across the adult lifespan, offering a framework by which a better understanding of the influences of DA modulation across the adult lifespan may be achieved.

STAR★METHODS

Detailed methods are provided in the online version of this paper and include the following:

- **KEY RESOURCES TABLE**
- **RESOURCE AVAILABILITY**
 - Lead contact
 - Materials availability
 - Data and code availability
- **EXPERIMENTAL MODEL AND STUDY PARTICIPANT DETAILS**
 - Participants
- **METHOD DETAILS**
 - Imaging procedures
 - PET imaging
 - MR imaging
 - Memory
- **QUANTIFICATION AND STATISTICAL ANALYSIS**

SUPPLEMENTAL INFORMATION

Supplemental information can be found online at <https://doi.org/10.1016/j.celrep.2023.113107>.

ACKNOWLEDGMENTS

This work was funded by Swedish Research Council grant 2016-01936 (A.S.), the Knut and Alice Wallenberg Foundation (A.S.), Riksbankens Jubileumsfond (A.S.), and a StratNeuro grant (A.S.).

AUTHOR CONTRIBUTIONS

Conceptualization, J.J. and A.S.; methodology, J.J., R.P., M.A., N.K., L.B., L.N., and A.S.; investigation, J.J., K.N., R.P., and A.S.; visualization, J.J.; supervision, A.S.; writing – original draft, J.J. and A.S.; writing – review & editing, J.J., K.N., R.P., N.K., G.P., M.A., S.M.K., K.R., M.G.-M., A.R., L.B., L.N., and A.S.

DECLARATION OF INTERESTS

The authors declare no competing interests.

INCLUSION AND DIVERSITY

We support inclusive, diverse, and equitable conduct of research.

Received: April 17, 2023

Revised: July 14, 2023

Accepted: August 22, 2023

REFERENCES

1. Li, S.C., Lindenberger, U., and Bäckman, L. (2010). Dopaminergic modulation of cognition across the life span. *Neurosci. Biobehav. Rev.* 34, 625–630. <https://doi.org/10.1016/j.neubiorev.2010.02.003>.
2. Wahlstrom, D., Collins, P., White, T., and Luciana, M. (2010). Developmental changes in dopamine neurotransmission in adolescence: Behavioral implications and issues in assessment. *Brain Cogn.* 72, 146–159. <https://doi.org/10.1016/j.bandc.2009.10.013>.
3. Reynolds, L.M., and Flores, C. (2021). Mesocorticolimbic Dopamine Pathways Across Adolescence: Diversity in Development. *Front. Neural Circuits* 15, 735625–735717. <https://doi.org/10.3389/fncir.2021.735625>.
4. Islam, K.U.S., Meli, N., and Blaess, S. (2021). The Development of the Mesoprefrontal Dopaminergic System in Health and Disease. *Front. Neural Circuits* 15, 746582. <https://doi.org/10.3389/fncir.2021.746582>.
5. Bäckman, L., Lindenberger, U., Li, S.C., Nyberg, L., Bäckman, L., Lindenberger, U., Li, S.C., and Nyberg, L. (2010). Linking cognitive aging to alterations in dopamine neurotransmitter functioning: Recent data and future avenues. *Neurosci. Biobehav. Rev.* 34, 670–677. <https://doi.org/10.1016/j.neubiorev.2009.12.008>.
6. Wahlstrom, D., White, T., Hooper, C.J., Vrshek-Schallhorn, S., Oetting, W.S., Brott, M.J., and Luciana, M. (2007). Variations in the Catechol O-methyltransferase Polymorphism and Prefrontally Guided Behaviors in Adolescents. *Biol. Psychiatry* 61, 626–632. <https://doi.org/10.1016/j.biopsych.2006.05.045>.
7. Klune, C.B., Jin, B., and Denardo, L.A. (2021). Linking mpfc circuit maturation to the developmental regulation of emotional memory and cognitive flexibility. *Elife* 10, 645677–e64633. <https://doi.org/10.7554/eLife.64567>.
8. Diamond, A., Briand, L., Fossella, J., and Gehlbach, L. (2004). Genetic and Neurochemical Modulation of Prefrontal Cognitive Functions in Children. *Am. J. Psychiatr.* 161, 125–132. <https://doi.org/10.1176/appi.ajp.161.1.125>.
9. Diamond, A., and Baddeley, A. (1996). Evidence for the importance of dopamine for prefrontal cortex functions early in life. *Philos. Trans. R. Soc. Lond. B Biol. Sci.* 351, 1483–1493.
10. Diamond, A. (2009). Normal Development of Prefrontal Cortex from Birth to Young Adulthood: Cognitive Functions, Anatomy, and Biochemistry. *Princ. Front. Lobe Funct.* <https://doi.org/10.1093/acprof:oso/9780195134971.003.0029>.
11. Lindenberger, U., Nagel, I.E., Chicherio, C., Li, S.C., Heekeren, H.R., and Bäckman, L. (2008). Age-Related Decline in Brain Resources Modulates Genetic Effects on Cognitive Functioning. *Front. Neurosci.* 2, 234–244. <https://doi.org/10.3389/neuro.01.039.2008>.
12. Nagel, I.E., Chicherio, C., Li, S.C., von Oertzen, T., Sander, T., Villringer, A., Heekeren, H.R., Bäckman, L., and Lindenberger, U. (2008). Human aging magnifies genetic effects on executive functioning and working memory. *Front. Hum. Neurosci.* 2, 1–8. <https://doi.org/10.3389/neuro.09.001.2008>.
13. Volkow, N.D., Gur, R.C., Wang, G.J., Fowler, J.S., Moberg, P.J., Ding, Y.S., Hitzemann, R., Smith, G., and Logan, J. (1998). Association between decline in brain dopamine activity with age and cognitive and motor

- impairment in healthy individuals. *Am. J. Psychiatr.* 155, 344–349. <https://doi.org/10.1176/ajp.155.3.344>.
14. Bäckman, L., Ph, D., Ginovart, N., Ph, D., Dixon, R.A., Ph, D., Wahlin, T.R., Sc, M., Wahlin, Å., Ph, D., et al. (2000). Age-Related Cognitive Deficits Mediated by Changes in the Striatal Dopamine System, pp. 635–637.
15. Bäckman, L., Nyberg, L., Lindenberger, U., Li, S.C., and Farde, L. (2006). The correlative triad among aging, dopamine, and cognition: current status and future prospects. *Neurosci. Biobehav. Rev.* 30, 791–807. <https://doi.org/10.1016/j.neubiorev.2006.06.005>.
16. Karalija, N., Wählin, A., Ek, J., Rieckmann, A., Papenberg, G., Salami, A., Brandmaier, A.M., Köhncke, Y., Johansson, J., Andersson, M., et al. (2019). Cardiovascular factors are related to dopamine integrity and cognition in aging. *Ann. Clin. Transl. Neurol.* 6, 2291–2303. <https://doi.org/10.1002/acn3.50927>.
17. Karrer, T.M., Josef, A.K., Mata, R., Morris, E.D., and Samanez-Larkin, G.R. (2017). Reduced dopamine receptors and transporters but not synthesis capacity in normal aging adults: a meta-analysis. *Neurobiol. Aging* 57, 36–46. <https://doi.org/10.1016/j.neurobiolaging.2017.05.006>.
18. Lidow, M.S., Goldman-Rakic, P.S., and Rakic, P. (1991). Synchronized overproduction of neurotransmitter receptors in diverse regions of the primate cerebral cortex. *Proc. Natl. Acad. Sci. USA* 88, 10218–10221. <https://doi.org/10.1073/pnas.88.22.10218>.
19. Seeman, P., Bzowej, N.H., Guan, H.-C., Bergeron, C., Becker, L.E., Reynolds, G.P., Bird, E.D., Riederer, P., Jellinger, K., Watanabe, S., et al. (1987). Human brain dopamine receptors in children and aging adults. *Synapse* 1, 399–404. <https://doi.org/10.1002/syn.890010503>.
20. Larsen, B., Olafsson, V., Calabro, F., Laymon, C., Tervo-Clemmens, B., Campbell, E., Minhas, D., Montez, D., Price, J., and Luna, B. (2020). Maturation of the human striatal dopamine system revealed by PET and quantitative MRI. *Nat. Commun.* 11, 846–910. <https://doi.org/10.1038/s41467-020-14693-3>.
21. Weickert, C.S., Webster, M.J., Gondipalli, P., Rothmond, D., Fatula, R.J., Herman, M.M., Kleinman, J.E., and Akil, M. (2007). Postnatal alterations in dopaminergic markers in the human prefrontal cortex. *Neuroscience* 144, 1109–1119. <https://doi.org/10.1016/j.neuroscience.2006.10.009>.
22. Rothmond, D.A., Weickert, C.S., and Webster, M.J. (2012). Developmental changes in human dopamine neurotransmission: Cortical receptors and terminators. *BMC Neurosci.* 13, 18. <https://doi.org/10.1186/1471-2202-13-18>.
23. Jucaite, A., Forsberg, H., Karlsson, P., Halldin, C., and Farde, L. (2010). Age-related reduction in dopamine D1 receptors in the human brain: From late childhood to adulthood, a positron emission tomography study. *Neuroscience* 167, 104–110. <https://doi.org/10.1016/j.neuroscience.2010.01.034>.
24. Shepherd, G.M.G. (2013). Corticostriatal connectivity and its role in disease. *Nat. Rev. Neurosci.* 14, 278–291. <https://doi.org/10.1038/nrn3469>.
25. Nordin, K., Gorbach, T., Pedersen, R., Panes Lundmark, V., Johansson, J., Andersson, M., McNulty, C., Riklund, K., Wählin, A., Papenberg, G., et al. (2022). DyNAmIC: A prospective longitudinal study of dopamine and brain connectomes: A new window into cognitive aging. *J. Neurosci. Res.* 100, 1296–1320. <https://doi.org/10.1002/jnr.25039>.
26. Hall, H., Sedvall, G., Magnusson, O., Kopp, J., Halldin, C., and Farde, L. (1994). Distribution of D1- and D2-dopamine receptors, and dopamine and its metabolites in the human brain. *Neuropsychopharmacology* 11, 245–256. <https://doi.org/10.1038/sj.npp.1380111>.
27. Jaber, M., Robinson, S.W., Missale, C., and Caron, M.G. (1996). Dopamine Receptors and Brain Function. *Neuropharmacology* 35, 1503–1519.
28. Rinne, J.O., Lönnberg, P., and Marjamäki, P. (1990). Age-dependent decline in human brain dopamine D1 and D2 receptors. *Brain Res.* 508, 349–352. [https://doi.org/10.1016/0006-8993\(90\)90423-9](https://doi.org/10.1016/0006-8993(90)90423-9).
29. Suhara, T., Fukuda, H., Inoue, O., Itoh, T., Suzuki, K., Yamasaki, T., and Tateno, Y. (1991). Age-related changes in human D1 dopamine receptors measured by positron emission tomography. *Psychopharmacology (Berl)* 103, 41–45. <https://doi.org/10.1007/BF02244071>.
30. Sowell, E.R., Peterson, B.S., Thompson, P.M., Welcome, S.E., Henkenius, A.L., and Toga, A.W. (2003). Mapping cortical change across the human life span. *Nat. Neurosci.* 6, 309–315. <https://doi.org/10.1038/nn1008>.
31. Fjell, A.M., Westlye, L.T., Grydeland, H., Amlie, I., Espeseth, T., Reinvang, I., Raz, N., Holland, D., Dale, A.M., and Walhovd, K.B.; Alzheimer Disease Neuroimaging Initiative (2013). Critical ages in the life course of the adult brain: Nonlinear subcortical aging. *Neurobiol. Aging* 34, 2239–2247. <https://doi.org/10.1016/j.neurobiolaging.2013.04.006>.
32. Karalija, N., Johansson, J., Papenberg, G., Wählin, A., Salami, A., Köhncke, Y., Brandmaier, A.M., Andersson, M., Axelsson, J., Riklund, K., et al. (2022). Longitudinal Dopamine D2 Receptor Changes and Cerebrovascular Health in Aging. *Neurology* 99, e1278–e1289. <https://doi.org/10.1212/wnl.000000000000200891>.
33. Ito, H., Takahashi, H., Arakawa, R., Takano, H., and Suhara, T. (2008). Normal database of dopaminergic neurotransmission system in human brain measured by positron emission tomography. *Neuroimage* 39, 555–565. <https://doi.org/10.1016/j.neuroimage.2007.09.011>.
34. Desikan, R.S., Ségonne, F., Fischl, B., Quinn, B.T., Dickerson, B.C., Blacker, D., Buckner, R.L., Dale, A.M., Maguire, R.P., Hyman, B.T., et al. (2006). An automated labeling system for subdividing the human cerebral cortex on MRI scans into gyral based regions of interest. *Neuroimage* 31, 968–980. <https://doi.org/10.1016/j.neuroimage.2006.01.021>.
35. Fischl, B. (2012). FreeSurfer. *Neuroimage* 62, 774–781. <https://doi.org/10.1016/j.neuroimage.2012.01.021>.
36. Schwarz, G. (1978). Estimating the Dimension of a Model. *Ann. Stat.* 6, 461–464. <https://doi.org/10.1214/aos/1176344136>.
37. Pedersen, E.J., Miller, D.L., Simpson, G.L., and Ross, N. (2019). Hierarchical Generalized Additive Models in Ecology: An Introduction with Mgc. *PeerJ*. <https://doi.org/10.7717/peerj.6876>.
38. Rieckmann, A., Hedden, T., Younger, A.P., Sperling, R.A., Johnson, K.A., and Buckner, R.L. (2016). Dopamine transporter availability in clinically normal aging is associated with individual differences in white matter integrity. *Hum. Brain Mapp.* 37, 621–631. <https://doi.org/10.1002/hbm.23054>.
39. Schmidt, P., Gaser, C., Arsic, M., Buck, D., Förschler, A., Berthele, A., Hoshi, M., Ilg, R., Schmid, V.J., Zimmer, C., et al. (2012). An automated tool for detection of FLAIR-hyperintense white-matter lesions in Multiple Sclerosis. *Neuroimage* 59, 3774–3783. <https://doi.org/10.1016/j.neuroimage.2011.11.032>.
40. Wardlaw, J.M., Smith, C., and Dichgans, M. (2013). Mechanisms of sporadic cerebral small vessel disease: Insights from neuroimaging. *Lancet Neurol.* 12, 483–497. [https://doi.org/10.1016/S1474-4422\(13\)70060-7](https://doi.org/10.1016/S1474-4422(13)70060-7).
41. D'Agostino, R.B., Vasan, R.S., Pencina, M.J., Wolf, P.A., Cobain, M., Mas-saro, J.M., and Kannel, W.B. (2008). General cardiovascular risk profile for use in primary care: The Framingham heart study. *Circulation* 117, 743–753. <https://doi.org/10.1161/CIRCULATIONAHA.107.699579>.
42. Tziortzi, A.C., Haber, S.N., Searle, G.E., Tsoumpas, C., Long, C.J., Shot-bolt, P., Douaud, G., Jbabdi, S., Behrens, T.E.J., Rabiner, E.A., et al. (2014). Connectivity-based functional analysis of dopamine release in the striatum using diffusion-weighted MRI and positron emission tomography. *Cerebr. Cortex* 24, 1165–1177. <https://doi.org/10.1093/cercor/bhs397>.
43. O'Rawe, J.F., and Leung, H.C. (2022). Topographic organization of the human caudate functional connectivity and age-related changes with resting-state fMRI. *Front. Syst. Neurosci.* 16, 966433. <https://doi.org/10.3389/fnsys.2022.966433>.
44. Rieckmann, A., Karlsson, S., Fischer, H., and Bäckman, L. (2011). Caudate dopamine D1 receptor density is associated with individual differences in frontoparietal connectivity during working memory. *J. Neurosci.* 31, 14284–14290. <https://doi.org/10.1523/JNEUROSCI.3114-11.2011>.

45. Nyberg, L., Karalija, N., Salami, A., Andersson, M., Wåhlin, A., Kaboovand, N., Köhncke, Y., Axelsson, J., Rieckmann, A., Papenberg, G., et al. (2016). Dopamine D2 receptor availability is linked to hippocampal-caudate functional connectivity and episodic memory. *Proc. Natl. Acad. Sci. USA* 113, 7918–7923. <https://doi.org/10.1073/pnas.1606309113>.
46. Bäckman, L., Karlsson, S., Fischer, H., Karlsson, P., Brehmer, Y., Rieckmann, A., MacDonald, S.W.S., Farde, L., and Nyberg, L. (2011). Dopamine D1 receptors and age differences in brain activation during working memory. *Neurobiol. Aging* 32, 1849–1856. <https://doi.org/10.1016/j.neurobiolaging.2009.10.018>.
47. Wen, X., He, H., Dong, L., Chen, J., Yang, J., Guo, H., Luo, C., and Yao, D. (2020). Alterations of local functional connectivity in lifespan: A resting-state fMRI study. *Brain Behav.* 10, 016522–e1710. <https://doi.org/10.1002/brb3.1652>.
48. Ystad, M., Eichele, T., Lundervold, A.J., and Lundervold, A. (2010). Subcortical functional connectivity and verbal episodic memory in healthy elderly-A resting state fMRI study. *Neuroimage* 52, 379–388. <https://doi.org/10.1016/j.neuroimage.2010.03.062>.
49. Barber, A.D., Sarpal, D.K., John, M., Fales, C.L., Mostofsky, S.H., Malhotra, A.K., Karlsgodt, K.H., and Lencz, T.; Pediatric Imaging, Neurocognition, and Genetics PING Study Consortium (2019). Age-Normative Pathways of Striatal Connectivity Related to Clinical Symptoms in the General Population. *Biol. Psychiatry* 85, 966–976. <https://doi.org/10.1016/j.biopsych.2019.01.024>.
50. Li, S.C., and Sikström, S. (2002). Integrative neurocomputational perspectives on cognitive aging, neuromodulation, and representation. *Neurosci. Biobehav. Rev.* 26, 795–808. [https://doi.org/10.1016/S0149-7634\(02\)00066-0](https://doi.org/10.1016/S0149-7634(02)00066-0).
51. Seaman, K.L., Smith, C.T., Juarez, E.J., Dang, L.C., Castrellon, J.J., Burgess, L.L., San Juan, M.D., Kundzic, P.M., Cowan, R.L., Zald, D.H., and Samanez-Larkin, G.R. (2019). Differential regional decline in dopamine receptor availability across adulthood: Linear and nonlinear effects of age. *Hum. Brain Mapp.* 40, 3125–3138. <https://doi.org/10.1002/hbm.24585>.
52. Antonini, A., and Leenders, K.L. (1993). Dopamine D2 Receptors in Normal Human Brain: Effect of Age Measured by Positron Emission Tomography (PET) and [11C]-Raclopride. *Ann. N. Y. Acad. Sci.* 695, 81–85. <https://doi.org/10.1111/j.1749-6632.1993.tb23033.x>.
53. Bakken, T.E., Miller, J.A., Ding, S.L., Sunkin, S.M., Smith, K.A., Ng, L., Szafer, A., Dalley, R.A., Royall, J.J., Lemon, T., et al. (2016). A comprehensive transcriptional map of primate brain development. *Nature* 535, 367–375. <https://doi.org/10.1038/nature18637>.
54. Iadecola, C. (2013). The Pathobiology of Vascular Dementia. *Neuron* 80, 844–866. <https://doi.org/10.1016/j.neuron.2013.10.008>.
55. Wang, L., Su, L., Shen, H., and Hu, D. (2012). Decoding Lifespan Changes of the Human Brain Using Resting-State Functional Connectivity MRI. *PLoS One* 7, e44530. <https://doi.org/10.1371/journal.pone.0044530>.
56. Bartzokis, G., Lu, P.H., Heydari, P., Couvrette, A., Lee, G.J., Kalashyan, G., Freeman, F., Grinstead, J.W., Villablanca, P., Finn, J.P., et al. (2012). Multimodal magnetic resonance imaging assessment of white matter aging trajectories over the lifespan of healthy individuals. *Biol. Psychiatry* 72, 1026–1034. <https://doi.org/10.1016/j.biopsych.2012.07.010>.
57. Raz, N., Lindenberger, U., Rodrigue, K.M., Kennedy, K.M., Head, D., Williamson, A., Dahle, C., Gerstorf, D., and Acker, J.D. (2005). Regional brain changes in aging healthy adults: General trends, individual differences and modifiers. *Cerebr. Cortex* 15, 1676–1689. <https://doi.org/10.1093/cercor/bhi044>.
58. Schaie, K.W. (1994). The course of adult intellectual development. *Am. Psychol.* 49, 304–313. <https://doi.org/10.1037/0003-066X.49.4.304>.
59. Rönnlund, M., Nyberg, L., Bäckman, L., and Nilsson, L.-G. (2005). Stability, Growth, and Decline in Adult Life Span Development of Declarative Memory: A Cross-Sectional and Longitudinal Data From a Population-Based Study. *Psychol. Aging* 20, 3–18. <https://doi.org/10.1037/0882-7974.20.1.3>.
60. Pedersen, R., Johansson, J., and Salami, A. (2023). Dopamine D1-signaling modulates maintenance of functional network segregation in aging. *Aging Brain* 3, 100079. <https://doi.org/10.1016/j.nbas.2023.100079>.
61. Tullberg, M., Fletcher, E., DeCarli, C., Mungas, D., Reed, B.R., Harvey, D.J., Weiner, M.W., Chui, H.C., and Jagust, W.J. (2004). White matter lesions impair frontal lobe function regardless of their location. *Neurology* 63, 246–253. <https://doi.org/10.1212/01.WNL.0000130530.55104.B5>.
62. Tubi, M.A., Feingold, F.W., Kothapalli, D., Hare, E.T., King, K.S., Thompson, P.M., and Braskie, M.N. (2020). White Matter Hyperintensities and Their Relationship to Cognition: Effects of Segmentation Algorithm. *Neuroimage* 206. <https://doi.org/10.1016/j.neuroimage.2019.116327>.
63. Guitart-Masip, M., Salami, A., Garrett, D., Rieckmann, A., Lindenberg, U., and Bäckman, L. (2016). BOLD Variability is Related to Dopaminergic Neurotransmission and Cognitive Aging. *Cerebr. Cortex* 26, 2074–2083. <https://doi.org/10.1093/cercor/bhv029>.
64. Haber, S.N. (2016). Corticostriatal circuitry. *Dialogues Clin. Neurosci.* 18, 7–21. <https://doi.org/10.31887/dcns.2016.18.1/shaber>.
65. Rieckmann, A., Johnson, K.A., Sperling, R.A., Buckner, R.L., and Hedden, T. (2018). Dedifferentiation of caudate functional connectivity and striatal dopamine transporter density predict memory change in normal aging. *Proc. Natl. Acad. Sci. USA* 115, 10160–10165. <https://doi.org/10.1073/pnas.1804641115>.
66. Dreher, J.C., Meyer-Lindenberg, A., Kohn, P., and Berman, K.F. (2008). Age-related changes in midbrain dopaminergic regulation of the human reward system. *Proc. Natl. Acad. Sci. USA* 105, 15106–15111. <https://doi.org/10.1073/pnas.0802127105>.
67. Berry, A.S., Shah, V.D., Baker, S.L., Vogel, J.W., O’Neil, J.P., Janabi, M., Schwimmer, H.D., Marks, S.M., and Jagust, W.J. (2016). Aging Affects Dopaminergic Neural Mechanisms of Cognitive Flexibility. *J. Neurosci.* 36, 12559–12569. <https://doi.org/10.1523/JNEUROSCI.0626-16.2016>.
68. Berry, A.S., Shah, V.D., and Jagust, W.J. (2018). The Influence of Dopamine on Cognitive Flexibility Is Mediated by Functional Connectivity in Young but Not Older Adults. *J. Cognit. Neurosci.* 30, 1330–1344. https://doi.org/10.1162/jocn_a_01286.
69. Sulzer, D., Cragg, S.J., and Rice, M.E. (2016). Striatal dopamine neurotransmission: Regulation of release and uptake. *Basal Ganglia* 6, 123–148. <https://doi.org/10.1016/j.baga.2016.02.001>.
70. Kaasinen, V., Vahlberg, T., Stoessl, A.J., Strafella, A.P., and Antonini, A. (2021). Dopamine Receptors in Parkinson’s Disease: A Meta-Analysis of Imaging Studies. *Mov. Disord.* 36, 1781–1791. <https://doi.org/10.1002/mds.28632>.
71. Klostermann, E.C., Braskie, M.N., Landau, S.M., O’Neil, J.P., and Jagust, W.J. (2012). Dopamine and frontostriatal networks in cognitive aging. *Neurobiol. Aging* 33, 623.e15–623.e24. <https://doi.org/10.1016/j.neurobiolaging.2011.03.002>.
72. Ciampa, C.J., Parent, J.H., Lapoint, M.R., Swinnerton, K.N., Taylor, M.M., Tennant, V.R., Whitman, A.J., Jagust, W.J., and Berry, A.S. (2022). Elevated Dopamine Synthesis as a Mechanism of Cognitive Resilience in Aging. *Cerebr. Cortex* 32, 2762–2772. <https://doi.org/10.1093/cercor/bhab379>.
73. Van Dyck, C.H., Seibyl, J.P., Malison, R.T., Laruelle, M., Zoghbi, S.S., Baldwin, R.M., and Innis, R.B. (2002). Age-related decline in dopamine transporters: Analysis of striatal subregions, nonlinear effects, and hemispheric asymmetries. *Am. J. Geriatr. Psychiatry* 10, 36–43. <https://doi.org/10.1097/00019442-200201000-00005>.
74. Ekelund, J., Slifstein, M., Narendran, R., Guillin, O., Belani, H., Guo, N.N., Hwang, Y., Hwang, D.R., Abi-Dargham, A., and Laruelle, M. (2007). In vivo DA D1 receptor selectivity of NNC 112 and SCH 23390. *Mol. Imaging Biol.* 9, 117–125. <https://doi.org/10.1007/s11307-007-0077-4>.
75. Beliveau, V., Ganz, M., Feng, L., Ozenne, B., Højgaard, L., Fisher, P.M., Svarer, C., Greve, D.N., Knudsen, G.M., Fisher, P.M., et al. (2017). A High-Resolution In Vivo Atlas of the Human Brain’s Serotonin System.

- J. Neurosci. 37, 120–128. <https://doi.org/10.1523/jneurosci.2830-16.2017>.
76. Karrer, T.M., McLaughlin, C.L., Guaglianone, C.P., and Samanez-Larkin, G.R. (2019). Reduced serotonin receptors and transporters in normal aging adults: a meta-analysis of PET and SPECT imaging studies. *Neurobiol. Aging* 80, 1–10. <https://doi.org/10.1016/j.neurobiolaging.2019.03.021>.
77. Greve, D.N., Salat, D.H., Bowen, S.L., Izquierdo-Garcia, D., Schultz, A.P., Catana, C., Becker, J.A., Svarer, C., Knudsen, G.M., Sperling, R.A., and Johnson, K.A. (2016). Different partial volume correction methods lead to different conclusions: An18F-FDG-PET study of aging. *Neuroimage* 132, 334–343. <https://doi.org/10.1016/j.neuroimage.2016.02.042>.
78. Lammertsma, A.A., and Hume, S.P. (1996). Simplified reference tissue model for PET receptor studies. *Neuroimage* 4, 153–158. <https://doi.org/10.1006/nimg.1996.0066>.
79. Ichise, M., Liow, J.S., Lu, J.Q., Takano, A., Model, K., Toyama, H., Suhara, T., Suzuki, K., Innis, R.B., and Carson, R.E. (2003). Linearized reference tissue parametric imaging methods: Application to [¹¹C]DASB positron emission tomography studies of the serotonin transporter in human brain. *J. Cereb. Blood Flow Metab.* 23, 1096–1112. <https://doi.org/10.1097/01.WCB.0000085441.37552.CA>.
80. Fischl, B., Salat, D.H., Busa, E., Albert, M., Dieterich, M., Haselgrove, C., Van Der Kouwe, A., Killiany, R., Kennedy, D., Klaveness, S., et al. (2002). Whole brain segmentation: Automated labeling of neuroanatomical structures in the human brain. *Neuron* 33, 341–355. [https://doi.org/10.1016/S0896-6273\(02\)00569-X](https://doi.org/10.1016/S0896-6273(02)00569-X).
81. Finn, E.S., Scheinost, D., Finn, D.M., Shen, X., Papademetris, X., and Constable, R.T. (2017). Can brain state be manipulated to emphasize individual differences in functional connectivity? *Neuroimage* 160, 140–151. <https://doi.org/10.1016/j.neuroimage.2017.03.064>.
82. Hallquist, M.N., Hwang, K., and Luna, B. (2013). The nuisance of nuisance regression: Spectral misspecification in a common approach to resting-state fMRI preprocessing reintroduces noise and obscures functional connectivity. *Neuroimage* 82, 208–225. <https://doi.org/10.1016/j.neuroimage.2013.05.116>.
83. Friston, K.J., Williams, S., Howard, R., Frackowiak, R.S., and Turner, R. (1996). Movement-related effects in fMRI time-series. *Magn. Reson. Med.* 35, 346–355. <https://doi.org/10.1002/mrm.1910350312>.
84. Power, J.D., Barnes, K.A., Snyder, A.Z., Schlaggar, B.L., and Petersen, S.E. (2012). Spurious but systematic correlations in functional connectivity MRI networks arise from subject motion. *Neuroimage* 59, 2142–2154. <https://doi.org/10.1016/j.neuroimage.2011.10.018>.
85. Glover, G.H., Li, T.Q., and Ress, D. (2000). Image-based method for retrospective correction of physiological motion effects in fMRI: RETROICOR. *Magn. Reson. Med.* 44, 162–167. [https://doi.org/10.1002/1522-2594\(200007\)44:1<162::AID-MRM23>3.0.CO;2-E](https://doi.org/10.1002/1522-2594(200007)44:1<162::AID-MRM23>3.0.CO;2-E).
86. Hutton, C., Josephs, O., Stadler, J., Featherstone, E., Reid, A., Speck, O., Bernarding, J., and Weiskopf, N. (2011). The impact of physiological noise correction on fMRI at 7T. *Neuroimage* 57, 101–112. <https://doi.org/10.1016/j.neuroimage.2011.04.018>.
87. Kasper, L., Bollmann, S., Diaconescu, A.O., Hutton, C., Heinze, J., Igleasias, S., Hauser, T.U., Sebold, M., Manjaly, Z.M., Pruessmann, K.P., and Stephan, K.E. (2017). The PhysIO Toolbox for Modeling Physiological Noise in fMRI Data. *J. Neurosci. Methods* 276, 56–72. <https://doi.org/10.1016/j.jneumeth.2016.10.019>.
88. Ashburner, J. (2007). A fast diffeomorphic image registration algorithm. *Neuroimage* 38, 95–113. <https://doi.org/10.1016/j.neuroimage.2007.07.007>.
89. Power, J.D., Cohen, A.L., Nelson, S.M., Wig, G.S., Barnes, K.A., Church, J.A., Vogel, A.C., Laumann, T.O., Miezin, F.M., Schlaggar, B.L., and Petersen, S.E. (2011). Functional Network Organization of the Human Brain. *Neuron* 72, 665–678. <https://doi.org/10.1016/j.neuron.2011.09.006>.
90. Choi, E.Y., Yeo, B.T.T., and Buckner, R.L. (2012). The organization of the human striatum estimated by intrinsic functional connectivity. *J. Neurophysiol.* 108, 2242–2263. <https://doi.org/10.1152/jn.00270.2012>.
91. Wood, S.N. (2017). Generalized Additive Models: An Introduction with R, second edition (Chapman and Hall/CRC). <https://doi.org/10.1201/9781315370279>.
92. Genolini, C., Ecochard, R., Benghezal, M., Driss, T., Andrieu, S., and Subtil, F. (2016). kmlShape: An efficient method to cluster longitudinal data (Time-Series) according to their shapes. *PLoS One* 11, 01507388–e150824. <https://doi.org/10.1371/journal.pone.0150738>.

STAR★METHODS

KEY RESOURCES TABLE

REAGENT or RESOURCE	SOURCE	IDENTIFIER
Software and algorithms		
FreeSurfer 6.0	Laboratories for Computational Neuroimaging (LCN), Athinoula A. Martinos Center for Biomedical Imaging, Boston, US	https://surfer.nmr.mgh.harvard.edu
Statistical Parametric Mapping (SPM12)	The Wellcome Center for Human Neuroimaging, UCL Queen Square Institute of Neurology, London, UK	https://www.fil.ion.ucl.ac.uk/spm/
MATLAB R2017	MathWorks, US	https://www.mathworks.com/products/matlab.html
RStudio Version 1.1.463	Posit Software, Boston, US	https://posit.co/download/rstudio-desktop/
Lesion Segmentation Tool Version 3.0.0	Paul Schmidt, Jena, Germany	https://www.applied-statistics.de/lst.html
Custom analysis code	Zenodo	https://doi.org/10.5281/zenodo.8274139
Other		
3 Tesla magnetic resonance imaging (MRI) device	General Electric, US	Discovery MR 750
Positron emission tomography (PET) device	General Electric, US	Discovery PET/CT 690

RESOURCE AVAILABILITY

Lead contact

Further information and requests for resources should be directed to and will be fulfilled by the lead contact, Jarkko Johansson (jarkko.johansson@umu.se).

Materials availability

This study did not generate new reagents.

Data and code availability

- Data used in this study will be available upon request with a completed Data Transfer Agreement.
- All original R analysis code has been deposited at Zenodo and made publicly available. DOIs are listed in the [key resources table](#).
- Any additional information required to reanalyze the data reported in this paper is available from the [lead contact](#) upon request.

EXPERIMENTAL MODEL AND STUDY PARTICIPANT DETAILS

We have reported the DyNAmIC study design, recruitment procedure, imaging protocols, cognitive testing and lifestyle questionnaires in detail elsewhere.²⁵ DyNAmIC is a prospective study of healthy individuals across the adult lifespan. Here, we restrict the description to the methodological and material aspects of direct relevance to the present study. The study was approved by the committees of Ethical and Radiation Safety, and all participants gave written informed consent prior to testing.

Participants

The sample was based on randomly selected invitees from the population registry of Umeå, Sweden. Responders were screened for exclusion criteria, including contraindications to magnetic imaging, mini mental state examination (MMSE) ≤ 25 , psychoactive medication, history of mental illness, and brain abnormalities. One hundred eighty ($n = 180$) volunteers were included in the study in an age- and sex-balanced manner across 20–80 y ($n = 30$ per decade, 50% female). 177 participants completed PET scanning using [^{11}C] SCH23390, but in one participant there were indications of subcutaneous injection leading to exclusion of this participant; other reasons for drop-out from PET were technical problems, and one participant declined to participate in PET.

METHOD DETAILS

Imaging procedures

Magnetic resonance (MR) imaging was conducted using a 3 tesla scanner (Discovery MR 750, General Electric), and a 32-channel phased-array head coil. PET scanning was conducted using a hybrid PET/CT system (Discovery PET/CT 690, General Electric). The planned time interval between the first and second study visit, including MR and PET scanning respectively, was within one to ten days. Actual range was 1–141 days. More specifically, the data collection proceeded as planned for the majority of subjects (range 1–10 days: for 83% of sample), and the scan interval was longer for the remaining 17% of participants (range 18–141 days).

PET imaging

Production of [^{11}C]SCH23390 was performed by the radiochemistry laboratory of Norrlands Universitetssjukhus, Umeå University. Target radioactivity in intravenous injections of [^{11}C]SCH23390 was 350 MBq (range = [205, 391] MBq, mean \pm sd = 337 ± 27 MBq, no significant differences across age-groups (age <40 and age \geq 40 y), Student's t-test $t = 0.79$, n.s.). Participants were positioned on the scanner bed in supine position, and individually fitted thermoplastic masks were used to prevent excessive head movement. Preceding the injection, a 5-min low-dose helical CT scan (20 mA, 120 kV, 0.8 s per revolution) was obtained for PET-attenuation correction. Continuous PET-measurement in list-mode format was initiated at the time of injection and continued for 60 min. Offline re-binning of list-mode data was conducted to achieve a sequence of time-framed data with increasing length: 6 \times 10, 6 \times 20, 6 \times 40, 9 \times 60, 22 \times 120 s (a total of 49 frames). Time-framed, attenuation-, scatter-, and decay-corrected PET images (47 slices, 25 cm field of view, 256 \times 256-pixel transaxial images, voxel size 0.977 \times 0.977 \times 3.27 mm³) were reconstructed using the manufacturer-supplied iterative VUE Point HD-SharpIR algorithm (6 iterations, 24 subsets, resolution-recovery).

Estimation of target binding potential (BP) relative to non-displaceable (BP_{ND}) binding as measured in the cerebellum was conducted according to procedures described previously.²⁵ Frame-to-frame head motion correction (translations range = [0.23, 4.22] mm, mean \pm sd = 0.95 ± 0.54 mm, a trend-level difference across age-groups (age <40 and age \geq 40 y), Student's t-test $t = 2.0$, $p = 0.047$, mean \pm sd young = 1.07 ± 0.52 , mean \pm sd old = 0.90 ± 0.55), and registration to T1-weighted MRIs were conducted by using Statistical Parametric Mapping software (SPM12, Wellcome Institute, London, UK), and corrected PET data were re-sliced to match the spatial dimensions of MR data (1 mm³ iso-tropic, 256 \times 256 \times 256). Partial-volume-effect (PVE) correction was achieved using the symmetric geometric transfer matrix (SGTM; regional correction) or Muller-Gartner (voxel-wise correction) method implemented in FreeSurfer,⁷⁷ and an estimated point-spread-function of 2.5 mm full-width-at-half-maximum (FWHM). Regional estimates of BP_{ND} were calculated within Desikan-Killiany cortical parcellation³⁴ and subcortical regions as provided in automated FreeSurfer segmentations (41 regions-of-interest), using the simplified reference tissue model (SRTM;⁷⁸). Voxel-wise estimates of BP_{ND} were calculated within gray-matter voxels (GM probability >0.9) using the multi-linear (simplified) reference tissue model (MRTM), with fixed k_2' (MRTM2;⁷⁹). Voxel-wise BP_{ND} maps were spatially normalized to match Montreal Neurological Institute (MNI) space using DARTEL-derived deformation fields. Cortical surface-reconstructions of BP_{ND} maps in MNI-space were conducted using FreeSurfer.

MR imaging

High-resolution anatomical T1-weighted images were collected using a 3D fast spoiled gradient-echo sequence. Imaging parameters were as follows: 176 sagittal slices, thickness = 1 mm, repetition time (TR) = 8.2 ms, echo-time (TE) = 3.2 ms, flip angle = 12°, and field of view (FOV) = 250 \times 250 mm. Anatomical T1-weighted images were used to parcel cortical and subcortical structures with the FreeSurfer 6.0 software (<https://surfer.nmr.mgh.harvard.edu>).⁸⁰ Striatal volumes were manually corrected using the Voxel Edit mode in Freeview when necessary.

Whole-brain functional images were acquired during naturalistic viewing (movie watching). During the fMRI session the participants were shown a 12 min clip of the Swedish comedy film called Cockpit (2012). The participants' reactions to the content of the movie were not monitored, but the clips were selected to be as neutral in their content as possible. The content of the movie: Following his termination as a pilot and the end of his marriage, Valle embarks on a quest to ensure a new employment. Faced with a desperation in the job market, he resorts to disguising himself as a woman with the intention of obtaining a position at a company specially seeking a female pilot. Furthermore, based on prior work, the strength of cortico-striatal connectivity was likely not heavily influenced by the state (rest, movie, n-back), whereas some previous work suggest that naturalistic viewing might be optimally sensitive to interindividual differences in connectivity.⁸¹ Functional images were sampled using a T2*-weighted single-shot echo-planar imaging (EPI) sequence, with a total of 350 volumes collected over 12 min. The functional sequence was sampled with 37 transaxial slices, slice thickness = 3.4 mm, 0.5 mm spacing, TR = 2000 ms, TE = 30 ms, flip angle = 80°, and FOV = 250 \times 250 mm.

fMRI preprocessing was carried out using the Statistical Parametric Mapping software package (SPM12; Wellcome Department of Imaging Science, Functional Imaging Laboratory). The functional images were first corrected for slice-timing differences, motion, and signal distortions and the time series were subsequently demeaned and detrended followed by simultaneous nuisance regression and temporal high-pass filtering (threshold at 0.009 Hz) in order not to re-introduce nuisance signals.⁸² Nuisance regressors included average CSF and WM time-series and their derivatives, 24-motion parameters,⁸³ a binary vector flagging motion-contaminated volumes exceeding framewise displacement (FD) of 0.2 mm,⁸⁴ in addition to an 18-parameter RETRICOR model^{85,86} of cardiac pulsation (up to third-order harmonics), respiration (up to fourth-order harmonics), and first-order cardio-respiratory interactions estimated

using the PhysIO Toolbox v.5.0⁸⁷. Nuisance-regressed images were subsequently normalized to a sample-specific group template (DARTEL;⁸⁸), spatially smoothed using a 6-mm FWHM Gaussian kernel and affine-transformed to stereotactic MNI space.

Functional connectivity (FC) graphs were created by correlating average time series sampled from 264 cortical locations⁸⁹ (5-mm spheres) in addition to two putative ROIs in the right and left associative caudate (MNI coordinates: right [10, 14, 2], left [-12, 12, 6]). Caudate seeds were selected to maximize preferential connectivity with task-positive networks.⁹⁰ Following Fisher's *r*-to-*z* transformation, a bilateral estimate of caudate FC strength was computed for each subject as the average sum of positive edge weights for the two vertices. Strength of frontoparietal connectivity was computed using a task-positive seed in the right prefrontal cortex (MNI coordinates: [36, 36, 26]) and age-sensitive posterior parietal cortex targets (MNI coordinates: [34, -62, 50], [60, -30, 34], [10, -70, 52], [-42, -52, 46]) identified in past research.⁴⁴

For assessment of white-matter hyperintensities, a fluid-attenuated inversion recovery (FLAIR) sequence was acquired. A total of 48 slices were obtained with a slice thickness of 3 mm, TE = 120 ms, TR = 8000 ms, TI = 2250 ms, and FOV = 240 x 240 mm. The lesion segmentation tool (LST; <https://www.applied-statistics.de/lst.html>) in SPM12 was used to segment white-matter lesions (hyperintensities in FLAIR). Segmentation was conducted using FLAIR, and T1 data and lesion growth algorithm (LGA).³⁹ Framingham Risk Scores (FRS)⁴¹ were used to assess the link between cardiovascular health and manifestation of white matter lesions. The Framingham Risk Score is a robust and extensively validated multivariable risk model employed to quantitatively assess the likelihood of a cardiovascular disease (CVD) event transpiring within a subsequent 10-year duration.⁴¹ We used the office-based version of the score, which is computed using age, sex, systolic blood pressure, blood pressure medication usage, body mass index, smoking status, and diabetes diagnosis as indicators. These indicators were aggregated into a multivariable CVD risk score per individual according to earlier descriptions.⁴¹

Memory

Tests of episodic memory included word recall, number-word recall, and object-location recall. In word recall, participants were presented with 16 words that appeared one by one on the computer screen. During the first phase, participants encoded each word for 6 s, and following presentation of all items in the series, participants used the keyboard to type in as many of the words they could recall, in any order. Performance was defined as the number of correctly recalled words. In number-word recall, participants were required to memorize pairs of 2-digit numbers and concrete plural nouns (e.g., 46 dogs). Ten number-word pairs were presented consecutively, each displayed for 6 s. Retrieval immediately followed, in which every word was consecutively presented again, but in a different order than during encoding. For object-location memory, participants encoded objects presented on different locations in a 6 x 6 square grid displayed on the computer screen. Each encoding trial involved 12 objects, presented one by one, in distinct locations within the grid. Each object-position pairing was displayed for 8 s before disappearing. Directly following encoding, all objects were simultaneously displayed next to the grid for participants to move them (in any order) to their correct location in the grid. A composite score of episodic memory (EPM) was computed. First, summary scores per task were computed across blocks or trials of tasks. Next, these summary scores were standardized (T-score: Mean = 50; SD = 10), and finally, a composite score was created by averaging the T-scored measures of each task.

Working memory was tested using three tasks, letter updating, number updating, and spatial updating. During letter updating, participants were presented with a sequence of capital letters (A–D), consecutively on the computer screen, requiring them to update and to keep the three lastly presented letters in memory. The letters were presented for 1 s, with an ISI of 0.5 s. When prompted, which could be at any given moment, participants provided their response by typing in three letters using the keyboard. Four practice trials were completed by all participants, followed by 16 test trials consisting of either 7-, 9-, 11-, or 13- letter sequences. The number-updating task had a columnized numerical 3-back design. Three boxes were present on the screen throughout the task, in which a single digit (1–9) was presented one at a time, from left to right during 1.5 s with an ISI of 0.5 s. During this ongoing sequence, participants had to judge whether the number currently presented in a specific box matched the last number presented in the same box (appearing three numbers before). Four test trials, each consisting of 30 numbers, followed after two practice trials. In the spatial-updating task, three 3 x 3 square grids were presented next to each other on the computer screen. At the beginning of each trial, a blue circular object was displayed at a random location within each grid. Following a presentation time of 4 s, the circular objects disappeared, leaving the grids empty. An arrow then appeared below each grid, indicating that the circular object in the corresponding grid was to be mentally moved one step in the direction of the arrow. The arrows appeared stepwise from the leftmost grid to the rightmost grid, each presented for 2.5 s (ISI = 0.5 s). The exercise of mentally moving the circular object was repeated one more time for each grid, prompted by three new arrows, resulting in the object having moved two steps from its original location at the end of each trial. Using the computer mouse, participants then indicated which square the circular object in each grid had ended up in. Performance was calculated as the sum of correct location indications across trials. A composite score of working memory (WM) was computed based on the three test scores, in the same way as described for EPM.

Finally, a composite score of memory function was calculated using principal component analysis (PCA) of WM and EPM scores across all participants (*n* = 176). Unrotated PCA loadings of the first component were 0.9 for both WM and EPM, and the first PC scores, explaining 80% of variance, were extracted to indicate memory function.

QUANTIFICATION AND STATISTICAL ANALYSIS

Generalized additive modeling (GAM;⁹¹) allowing for smooth functions was used as the primary age model, and model comparisons using Akaike information criteria (AIC;³⁶) were conducted to decide which model had most empirical support. Past research has predominantly considered linear and exponential decay D1DR – age models,^{17,29} the latter reflecting a non-linear, but monotonous, function of constant decay in relation to the concentration, whereas the preceding model is a good approximation of such decay when the decay rate (λ) is very low. Here, we hypothesized non-monotonous non-linear relationships between age and D1DR, which are poorly characterized by linear or exponential decay models. Conformity to the exponential-decay model was assessed using log-transformed D1DR availability and a linear model.

All ROI-level analysis were conducted using R (version 4.0.3). Univariate outliers in regional D1DR availability were searched and removed within each decade and sex ($n \approx 15$), by using the box-plot method (version 4.0.3). Outlier BP_{ND} were generally related to poor PET-model fit, and bilateral exclusion of BP_{ND} was present in less than 1% of the aggregate ROIs. R-package mgcv (version 1.8–33) was used for GAM analysis, and smoother functions in D1DR – age models were configured with six ($k = 6$) initial thin-plate (tp) basis functions, to avoid overfitting (method = REML, family = Gaussian). Function gam.check() was used to ensure the adequacy of the chosen basis dimensions. Complexity of the smoothers were penalized,⁹¹ and the resulting effective degrees of freedom were allowed to vary across regions. R-package gratia (version 0.6.0) was used for computation of GAM derivatives (1st and 2nd order) and the corresponding confidence intervals (CI 95%). Hierarchical (multivariate) GAMs³⁷ were constructed for the purpose of 1) dimension reduction in cortical ROIs; and 2) testing interregional differences in absence and presence of covariates. For the first, an HGAM including cortical D1DR availability (34 ROIs) as the dependent variable, and a global (fixed) effect of smooth age, regional (random) effects of intercept and smooth age, and a random effect of individual (intercept) as predictors was constructed. In this model, the global effect of age from cortical age trajectories was regressed out, and residual regional age effects were piped into a shape-respecting K-means clustering algorithm (R-package kmlShape, version 0.9.5;⁹²), to find regions sharing similar trajectories. Number of clusters were empirically optimized at $k = 3$. For the second, HGAMs were configured across regions (pairs), where the preceding analysis had suggested regionally-variant age trajectories; using a likelihood-ratio test, a model with a regional (random) effect of smooth age beyond a common smooth effect of age was compared to the common age-effect model. A significant result ($p < 0.05$) in the likelihood-ratio test indicated regional differences in age trajectories.³⁷ Furthermore, regional (random) effects of additional predictors (WML, GM, WM volumes) were used to test the persistence of regionally-variant age effects in the presence of regionally-variant exogenous predictors. Contributions of additional variables to regional D1DR differences beyond the effects of age were investigated using stepwise linear model comparisons assessing improvement in the model if the candidate variable was included (likelihood-ratio test, $p < 0.05$). Shapiro-Wilk normality tests (skewness, kurtosis) were conducted, and log-transformed variables were used to ensure normally distributed variables when needed.

Percent D1DR difference per decade was used as a measure of reduction rate:

$$\% \text{ D1DR difference per decade} = 100 \% \left(\frac{BP_x}{BP_y} - 1 \right) / \text{decades},$$

where BP_x is the BP_{ND} predicted at age x . R-package boot (version 1.3–25) was used for bootstrap-based estimation of the confidence interval % for D1DR differences per decade ($n = 500$ repetitions, CI 95% was used⁵¹).

Voxel-wise PET analyses were conducted using MATLAB (version 2017, Mathworks, US). Bilinear age-models were fit using a piecewise-linear least-squares algorithm (<https://www.mathworks.com/matlabcentral/fileexchange/40913-piecewise-linear-least-square-fit>). Prior to model fit, voxel-wise maps of D1DR availability were smoothed using an edge-preserving Gaussian smoothing kernel (FWHM = 8 mm). Voxel-wise statistical parametric maps were estimated using SPM12 for confirmatory analysis. Specifically, T-maps in young (age <40 y) and older (age ≥ 40 y) individuals were calculated to explore voxels showing a significant D1DR-memory association across the entire brain. A mask based on average T1 FreeSurfer parcellation in MNI-space was employed. Threshold $p < 0.01$ (uncorrected, cluster forming threshold $k = 50$) was used.

Multiple linear regression analysis were conducted in R to investigate the interrelations among age groups, D1DR availability, functional connectivity, and memory scores. Models were constructed to interrogate moderation of the effects of independent variables by age segment, e.g.: $DV \sim IV \times (\text{age} < 40)$, where DV is one of D1DR, FC or memory, and IV is one of age, D1, FC or their composite. Model improvement was quantified using $\Delta R^2 = R^2_{\text{moderated}} - R^2_{\text{unmoderated}}$, where moderated refers to the aforementioned age-segment moderated model and unmoderated is a simple linear model, and the significance of model improvement was assessed using an F-test between the nested models (anova() function in R). If significant moderation was detected, further analysis within the two age segments were conducted and Pearson's correlation was used to assess the significance, direction, and magnitude of the age-specific effects. Firstly, moderation of the age effect across two age segments was interrogated for D1, FC and memory, to assess the basic assumption of age differential implications of chronological age in early and late adulthood. When a significant interaction effect was detected (cf. above) this was included in subsequent analysis (e.g., $\text{memory} \sim \text{age} + \text{age} \times (\text{age} < 40)$ is the

appropriate base model for memory). Next, age-differential implications of D1DR to memory and functional connectivity were investigated by augmenting the base models of each dependent variable [e.g., $\text{memory} \sim \text{age} + \text{age} \times (\text{age} < 40) + \text{D1DR} + \text{D1DR} \times (\text{age} < 40)$], and model comparisons were conducted to assess the significance of age segment moderation. Finally, composite effects of D1DR and FC to memory were investigated in terms of moderation by age segment, and within each age segment separately [e.g., $\text{memory} \sim \text{D1DR} \times \text{FC}$, when $\text{age} < 40$]. Due to reduced sample size in age-split analysis ($\text{age} < 40$, $n = 55$), moderation analyses must be interpreted with caution.